JOURNAL OF CATALYSIS 121, 110–121 (1990)

Oxidative Coupling of Methane

I. Behavior and Characteristics of Pb–Mg–O Catalysts

S. K. AGARWAL, R. A. MIGONE, AND G. MARCELIN[1]

Chemical and Petroleum Engineering Department, University of Pittsburgh, Pittsburgh, Pennsylvania 15261

Received June 28, 1989; revised August 30, 1989

The role of the lead active species has been studied for Pb–Mg–O catalysts in the oxidative coupling of methane. In general, the effect of adding lead to MgO was to increase the rate of total methane conversion. The C_2 selectivity exhibited a volcano-type pattern with a maximum of 51% being achieved at about 0.4 at.% Pb. This volcano-type behavior is interpreted in terms of an "isolated site"-type mechanism. Addition of PbO in small amounts to a relatively inert MgO matrix results in the formation of a number of isolated strong oxidizing sites which can generate the methyl radicals more efficiently. Since these sites are isolated, the methyl radical has little likelihood of being further oxidized and can desorb into the gas phase where it can couple to form ethane. Surface and bulk characterization studies of the catalysts suggest that at low loadings the lead is indeed highly dispersed on the surface of the catalyst.

INTRODUCTION

The large amounts of natural gas (mainly methane) found worldwide has led to extensive recent research programs in the area of direct methane conversion. Although many routes are conceptually possible, the oxidative coupling of methane appears to offer short-term promise for directly converting methane to useful products without extensive energy consumption (*1*). In this process, methane is coupled to higher hydrocarbons by reacting it with a metal oxide, the reduced oxide being then oxidized by gas-phase oxygen in a catalytic cycle.

Although a number of different bulk and supported metal oxides have been found useful for the production of higher hydrocarbons (*2–7*), little is known about the nature of the surface or the active sites in many of these catalysts. Methane coupling is purported to take place by the abstraction of a hydrogen atom from a methane molecule giving $CH_3\cdot$ radical which can desorb into the gas phase and combine with another $CH_3\cdot$ radical to give ethane (*8, 9*). The competing reactions of $CH_3\cdot$ radicals, both on the surface and in the gas phase, to form CO_x largely control the selectivity to higher hydrocarbons.

Among the many metal oxides that have been studied, lead oxide and supported lead oxide have been reported to be suitable for the oxidative coupling of methane (*10, 11*). The support used plays an important role in controlling the C_2 selectivity with basic carriers such as MgO and β''-Al_2O_3 reportedly giving the highest C_2 selectivity. Asami *et al.* have reported a methane conversion of 13% and a C_2 selectivity of 71% at 800°C using a 20 wt% Pb–Mg–O catalyst (*12*).

This paper reports a study of the oxidative coupling of methane over a series of Pb–Mg–O catalysts with the goal of characterizing the bulk and surface nature of the material and studying the evolution of active sites as the chemical composition changes. These changes can be qualitatively explained by assuming isolated sites on the surface.

EXPERIMENTAL

The catalysts were prepared starting with lead (II) nitrate (99%) and MgO (99.5%) ob-

[1] To whom correspondence should be addressed.

0021-9517/90 $3.00

tained from Alfa Products. Catalysts containing 0.2, 0.4, 0.8, 2.6, 4.4, and 7.3 at.% Pb on magnesia were prepared by adding MgO to a $Pb(NO_3)_2$ solution of the appropriate concentration and evaporating to dryness. The catalysts were dried at 120°C and calcined, at 500°C for 15 h, followed by 750°C for 4 h, and finally 800°C for 4 h.

The BET surface areas of the catalysts were determined by N_2 physisorption at −196°C using a Micromeritics 2600 system. X-ray diffraction (XRD) measurements were taken with a General Electric XRD-5 diffractometer using Cu $K\alpha$ radiation. The lead and magnesium contents of the catalysts were determined by inductively coupled plasma (ICP) emission spectroscopy using a ARL ICP/AES Model 34000. The samples were digested in a 20% HNO_3 solution prior to ICP analyses.

X-ray photoelectron spectroscopy (XPS) measurements were obtained using a Perkin–Elmer Physical Electronics Model 550 surface analysis system. A PDP 11/04 computer (Digital Equipment Corp.) was used for collecting and analyzing the data. Powder samples were pressed onto adhesive tape strips which were introduced in the spectrometer chamber and outgassed at room temperature until reaching a pressure of 10^{-8} Torr. The samples were analyzed using a Mg $K\alpha$ 300-W source. The experimental spectra were collected for 30 min to 2 h, depending on the peak intensities, under high-resolution conditions (pass energies 25 eV). The peak areas were determined after smoothing and background subtraction of the spectra. The contaminant C 1*s* peak at 284.6-eV binding energy value was used as a reference to determine the binding energies of other elements. The Pb 4*f* transition, which consists of a strong doublet $4f_{7/2}$ and $4f_{5/2}$ separated by 4.9 ± 0.2 eV, the Mg 2*p* and 2*s*, and the O 1*s* peaks were measured. The concentration, C_x, of each element was calculated as:

$$C_x = \frac{[I_x/f_x]}{\sum_i [I_i/f_i]} \times 100, \qquad (1)$$

where I is the peak intensity and f is a sensitivity factor which accounts for the variation of the electron escape depth and detection efficiency of the detector with the kinetic energy of the electrons (*13*).

Electron microscopy analyses were performed on samples which had been prepared by suspending finely ground catalyst powder in *n*-pentane and spraying it on carbon film supported on a copper grid. A Jeol 2000 FX electron microscope was used for STEM studies. The particles were imaged using bright field technique.

The coupling reaction was studied using a laboratory scale fixed-bed reactor system operating under atmospheric pressure. The reactor was a quartz tube of 5 mm inner diameter tapered to 1 mm after the catalyst zone. The complete reactor system has been described previously (*2*). The gases methane (99.97%), oxygen (99.6%), and helium (99.995%) were obtained from Matheson and were further purified by passing through beds of indicating drierite and molecular sieves (5A).

The reaction conditions used were as follows: temperature = 780°C, reaction gas composition: $CH_4/O_2/He$ = 9/2/7, and pressure = 1 atm. The space velocity ranged between 1200 to 1513 cc/min/g. The catalyst was used in the form of 16/28-mesh pellets. In general, 150 mg of the catalyst was charged in the reactor. The effluent gases were analyzed by online GC, using Porapak-Q and molecular sieves (5A) columns, for methane, oxygen, carbon monoxide, carbon dioxide, ethane, ethylene, propane, propylene, and water.

The compositions of the catalysts are expressed in atomic percent in this paper. The methane conversion was calculated on the basis of total carbon balance. Selectivity is defined as the ratio of yield to methane conversion. The main products formed were ethane, ethylene, CO, CO_2, and H_2O. Some C_3 hydrocarbons were also formed with a selectivity of less than 2%, hence they are not reported.

TABLE 1

Binding Energies of Pb 4*f* and O 1*s* Electrons for Pb–Mg Catalysts

Catalyst	Binding energies (eV)					
	Pb $4f_{7/2}$		Pb $4f_{5/2}$		O 1*s*	
	Before reaction	After reaction	Before reaction	After reaction	Before reaction	After reaction
0.4% Pb–Mg	140.5	—	145.5	—	531.6	—
					533.6	—
0.8% Pb–Mg	141.1	140.9	145.9	145.7	530.1	
					532.4	532.6
					534.5	534.8
2.6% Pb–Mg	140.7	140.3	145.5	145.2	530.2	
					531.9	532.0
					533.9	534.0
4.4% Pb–Mg	140.7	140.3	145.6	145.1	529.4	530.4
					532.1	532.0
					534.3	534.0
7.3% Pb–Mg	140.6	140.7	145.4	145.6	529.8	529.7
					531.9	532.6
					534.1	534.9
PbO	139.4	—	144.3	—	531.7	—
					533.0	
Pb_3O_4	139.1	—	143.9	—	531.9	—
PbO_2	136.2	—	141.0	—	527.7	—
					529.2	
$PbCO_3$	140.4	—	145.3	—	530.5	—
					533.0	

RESULTS

Catalyst Characterization

The chemical nature of the catalysts was analyzed by bulk and surface-sensitive techniques both before and after the reaction. X-ray diffraction revealed the catalysts to consists of mixed PbO and MgO phases. The XRD patterns of the catalysts with low loadings of lead (<0.8% Pb) did not show any measurable PbO peaks. After reaction, XRD analyses of the catalysts which initially exhibited PbO peaks showed a decrease in the intensity of the PbO peaks relative to the MgO peaks, suggesting a loss of the PbO phase during the reaction. The XRD patterns did not show the formation of any Pb–Mg–O compounds. However, the presence of these compounds, either in trace amounts or in an amorphous form, cannot be totally ruled out.

Table 1 summarizes the Pb 4*f* and O 1*s* binding energies obtained by XPS of the different Pb–Mg–O catalysts. Corresponding values for some standard lead compounds, taken under the same conditions, are also shown for comparison. The Pb 4*f* peak consisting of a well-separated spin–orbit doublet is shown in Fig. 1 for different Pb oxides, $PbCO_3$, and the 0.4% Pb–Mg–O catalyst. For all the Pb–Mg–O catalysts, the measured Pb 4*f* binding energies were much higher than the corresponding energies for any of the lead oxides. However, both the Pb $4f_{7/2}$ and Pb $4f_{5/2}$ binding energies for the catalysts compare very well with $PbCO_3$, suggesting that lead is initially present in the form of $PbCO_3$ on the sur-

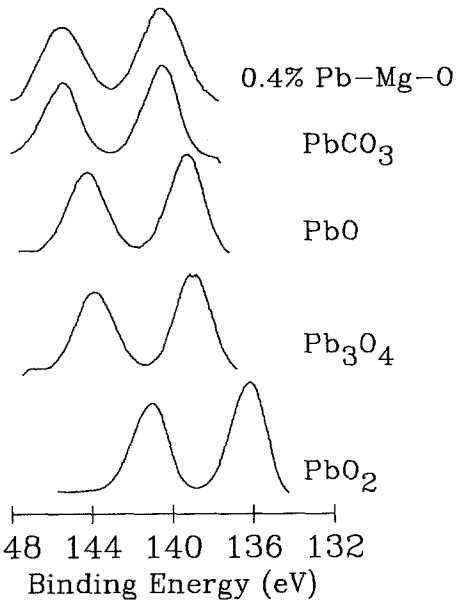

FIG. 1. XPS spectra showing the Pb $4f_{7/2}$ and $4f_{5/2}$ binding energies for 0.4% Pb–Mg–O, $PbCO_3$, and different lead oxides.

face. Previously reported values for the Pb 4*f* binding energies have shown some variability. For example, Kim *et al.* (*14*) have reported values of 137.5 and 137.9 for Pb $4f_{7/2}$ in PbO_2 and PbO, respectively, Jorgensen (*15*) reported 142.4 and 144.2, and Thomas and Tricker (*16*) have reported 137.6 and 138.8 for PbO_2 and PbO, respectively. However, the Pb 4*f* binding energy for $PbCO_3$ is reported to be higher than for the lead oxides (*15*), suggesting the presence of $PbCO_3$ in our catalysts. It is, however, difficult to rule out the presence of any Pb–Mg–O compounds on the catalyst surface as some compounds may have binding energies comparable to $PbCO_3$. The Mg 2*s* and 2*p* levels binding energy for MgO and Pb–Mg–O catalysts are shown in Table 2. In all cases, the Mg 2*p* binding energy was found to be 51.4 ± 0.3 eV, close to the measured value in MgO and in close agreement with the value of 51.1 ± 0.1 eV in MgO reported by Inoue and Yasumori (*17*).

As can be seen from Tables 1 and 2, the binding energies for each element were found to be almost independent of the PbO content of the catalysts. For most of the catalysts, the O 1*s* peak could be deconvoluted into three peaks. The peak at lower binding energy was assigned to the oxygen in $PbCO_3$, the center peak to the oxide ions within the structure of MgO, and the peak at the highest binding energy to oxygen containing surface contaminants such as adsorbed water or OH^- (*17*).

From XPS and atomic absorption analyses, the amounts of Pb on the surface and in the bulk of the catalysts were determined, respectively. These are summarized in Table 3. The amount of Pb in the bulk was found to increase from 0.4 to 6% as the nominal Pb content was increased from 0.4 to 7.3%. During the calcination step, the catalysts did not lose much Pb except in the

TABLE 2

Binding Energies of Mg 2*s* and 2*p* Electrons for Pb–Mg Catalysts

Catalyst	Binding Energies (eV)			
	Mg 2*s*		Mg 2*p*	
	Before reaction	After reaction	Before reaction	After reaction
MgO	90.5	—	51.7	—
0.4% Pb–Mg	89.9	—	51.1	—
0.8% Pb–Mg	90.8	90.6	52.0	51.9
2.6% Pb–Mg	90.3	90.2	51.5	51.4
4.4% Pb–Mg	90.4	90.0	51.6	51.3
7.3% Pb–Mg	90.3	90.7	51.5	52.0

TABLE 3

Bulk and Surface Composition of Pb–Mg Catalysts

Catalyst At.% Pb	At.% Pb			
	Before reaction (bulk)	After reaction (bulk)	Before reaction (surface)	After reaction (surface)
0.4% Pb–Mg	0.4	0.3	2.7	—
0.8% Pb–Mg	0.8	0.7	4.0	4.0
2.6% Pb–Mg	1.5	0.9	7.3	4.2
4.4% Pb–Mg	3.6	1.9	10.4	7.2
7.3% Pb–Mg	6.0	2.8	13.3	6.5

case of the catalysts with high lead content (>0.8 at.%). However, after the reaction, the lead content in the bulk decreased significantly for catalysts above 0.8% Pb. In all cases, the surface was found to be enriched with Pb species both before and after reaction.

Bright field STEM micrographs of the Pb–Mg–O catalysts showed significant differences depending on the loading of Pb. Whereas catalysts with low Pb content, i.e., less than 2.6%, showed only magnesium-rich regions, those with higher lead content exhibited notable variations in the elemental composition over various regions examined. Figure 2 shows a STEM micrograph for the 4.4% Pb–Mg–O catalyst. X-ray spectra from the regions marked are also shown in Fig. 2. In addition to the Cu signal generated by the microscope grid, a Mg$K\alpha$ signal and a Pb$M\alpha$ signal are distinctly observed in the spectra. Some regions were found to be highly enriched with lead while other regions consisted mainly of magnesium with small amounts of lead. Shown in Fig. 3 is a similar micrograph for the 0.4% Pb–Mg–O catalyst along with an X-ray spectrum of the marked region. This

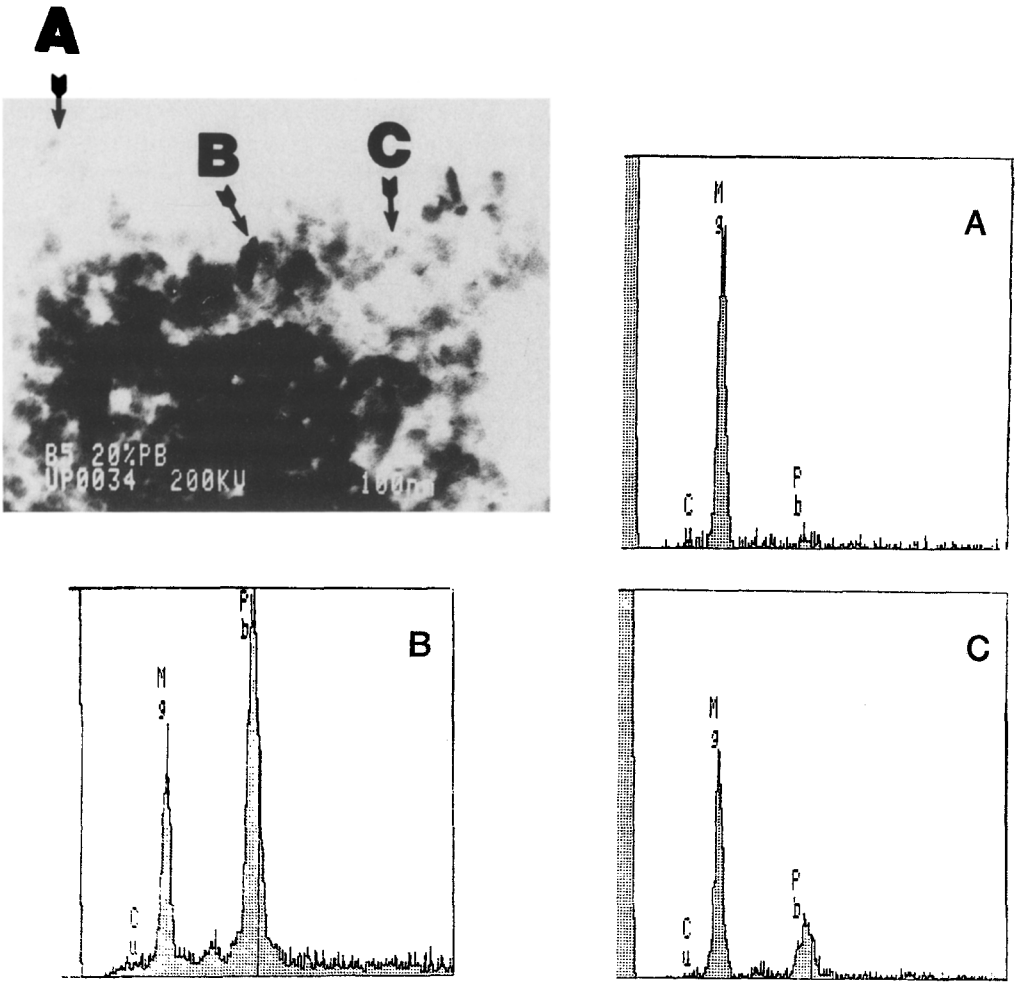

FIG. 2. Bright field STEM image of 4.4% Pb–Mg–O catalyst. X-ray spectra from different regions, marked in the image, are shown in A, B, and C.

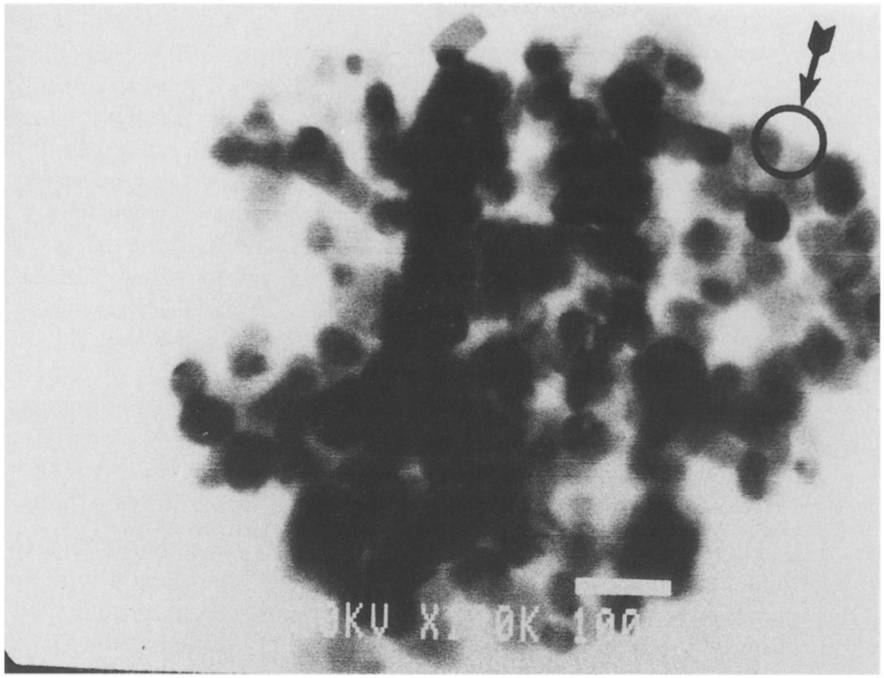

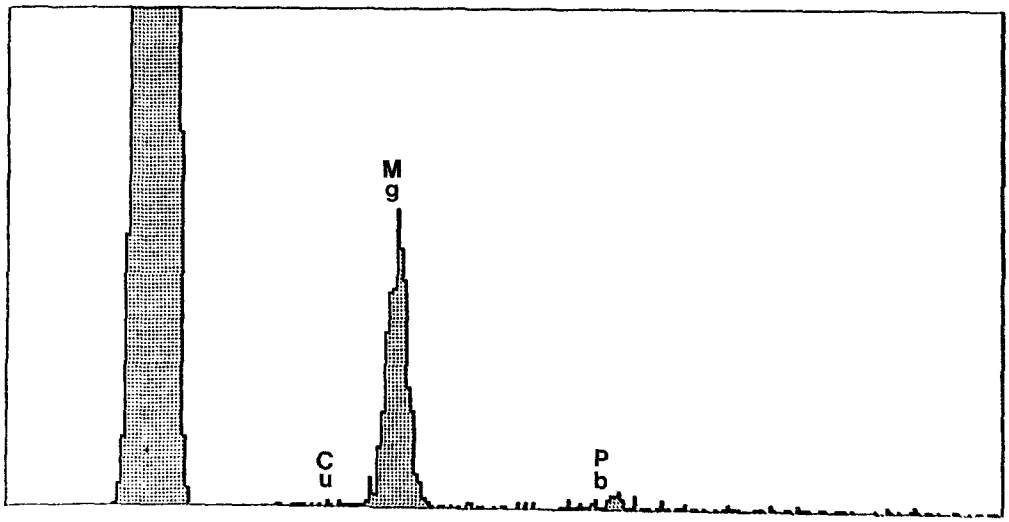

FIG. 3. Bright field STEM image of 0.4% Pb–Mg–O catalyst. X-ray spectrum from the marked region is also shown.

spectrum, which was typical over the entire surface examined, showed very low levels of lead, suggesting that in this catalyst the lead is uniformly distributed over the surface.

Reaction Studies

Because of the relatively high temperature involved in the oxidative coupling of methane a number of recent works have

TABLE 4

Surface and Catalytic Properties of Pb–Mg–O Catalysts at 780°C

Catalyst	BET surface area (m^2/g)		Space velocity (cc/min g)	% Methane conversion[a]	% Selectivities[a]		CO_2/CO[a]	Pseudo-specific rate[b] 10^{17} (molec/sec m^2)
	Before reaction	After reaction			C_2	CO_x		
MgO	36	25	1513	8.7	27.2	72.8	0.7	8.2
0.2% Pb–Mg	30	—	1513	12.8	42.6	56.4	0.9	14.4
0.4% Pb–Mg	28	19	1513	13.1	51.0	47.6	2.4	15.8
0.8% Pb–Mg	23	19	1200	13.9	46.0	51.3	9.3	16.3
2.6% Pb–Mg	14	13	1200	10.8	38.0	60.0	11.7	20.7
4.4% Pb–Mg	11	9	1200	10.4	20.0	78.8	26.3	25.4
7.3% Pb–Mg	11	7	1200	10.5	20.0	78.8	55.2	25.6

Note. Catalyst weight = 150 mg.

[a] Steady-state measurements were conducted after ca. 5 h on-stream.

[b] Based on initial surface area.

considered the importance of gas-phase contribution in this reaction (*2, 18–22*). To determine the noncatalytic gas-phase methane oxidation, the reaction was run in the absence of the catalyst. Total methane conversion, in the gas phase, was always less than 0.2% at temperatures up to 800°C. The very low methane conversion in the gas phase was due to the use of a tapered reactor which considerably reduced the exit volume and resulted in a very low residence time (~0.2 s) in the heated zone.

The steady-state catalytic properties of the different catalysts at 780°C are summarized in Table 4. The support, MgO, showed some activity but poor C_2 selectivity. These results are consistent with the data of Ross and co-workers, which reported a C_2 selectivity of 31% and a methane conversion of 7% at a temperature of 760°C (*23*). Other workers have reported different values for methane conversion and C_2 selectivity over MgO (*12, 24, 25*), but this disagreement is most likely due to the different catalyst preparation procedures and operating conditions employed in these various works.

An obvious effect of adding Pb to the MgO was an increase in activity for the conversion of methane. Perhaps most importantly, the addition of PbO in even small amounts to MgO resulted in a sharp increase in the C_2 selectivity. This C_2 selectivity exhibited a volcano-type behavior with maximum selectivity achieved at low loadings of PbO, about 0.4% Pb. This behavior is in accordance with the results of Asami *et al.* who reported a similar C_2 selectivity pattern exhibiting a maximum of 72% C_2 selectivity at 5 wt% (i.e., 0.4 at.% Pb) PbO, at a temperature of 750°C (*12*). Unfortunately, it was not possible to conduct the reaction over pure PbO, as some lead species were vaporized during reaction and plugged the reactor by condensing in the colder regions of the exit.

Two other major effects were observed upon the addition of PbO to MgO. First, the ratio of CO_2/CO produced was found to increase drastically and monotonically with increasing lead content. This ratio changed from 0.7 for pure MgO to 55 for 7.3% Pb–Mg–O. Secondly, when the reaction rate is expressed in terms of pseudo-specific areal rate (the term pseudo-specific needs to be emphasized since the reaction was not run under true differential condition), taking into account the initial surface area of the catalyst or the surface area after reaction, the specific activity was found to first increase monotonically and then level off with increasing lead content. Although the same general trend is observed with both sets of surface area numbers, a comparison

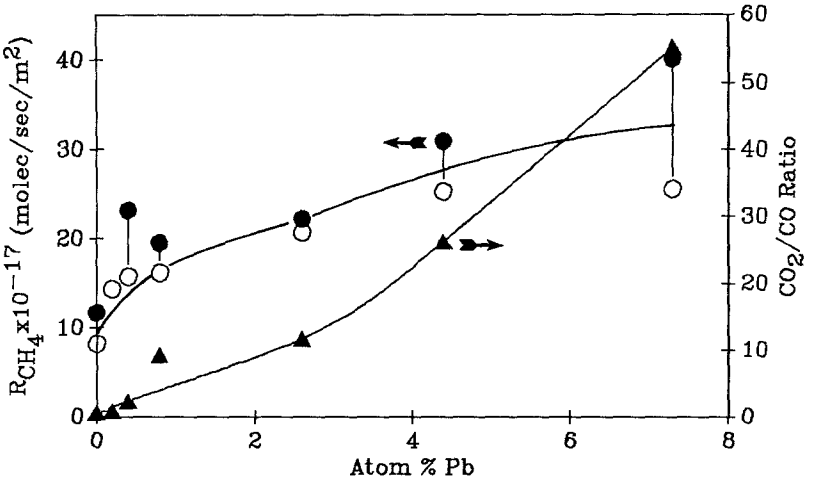

FIG. 4. Effect of lead content on the rate of overall methane conversion and CO_2/CO ratio for Pb–Mg–O catalysts. Open circles represent areal rate of methane conversion based on before reaction surface area, while closed circles represent areal rate of methane conversion based on after reaction surface area.

of rates based on the surface area after reaction may be somewhat misleading since all catalysts did not necessarily proceed through the same reaction-temperature history. These trends are depicted in Fig. 4.

Figure 5 shows the effect of time-on-stream for a 0 8% Pb–Mg–O catalyst at 780°C. This deactivation trend was typical of all catalysts studied. In general, methane conversion decreased with time; however, the Pb–Mg–O catalysts showed only a very slight deactivation when compared with other reported catalysts such as Sb–O (*2*). It should also be noted that for all Pb–Mg–

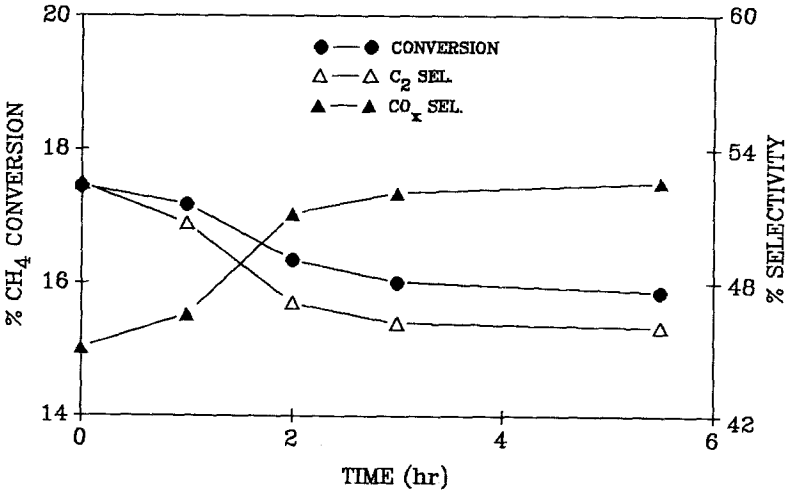

FIG. 5. Activity and selectivity variation with time-on-stream in methane coupling reaction over 0.8% Pb–Mg–O catalyst at 780°C.

O catalysts, C_2 selectivity decreased with time. In contrast, bare MgO catalyst did not show any appreciable deactivation.

DISCUSSION

The addition of Pb to MgO resulted in changes in both the activity and C_2 selectivity of the catalysts for the oxidative coupling of methane. Since the BET surface areas of the catalysts decreased with Pb content, this decrease should be accounted for while considering changes in the activity of the catalysts. Thus, when activity is reported in terms of a pseudo-specific rate, i.e., per unit surface area, the overall methane conversion was seen to increase with PbO loading. The leveling of the rate of methane conversion which was observed for catalysts containing higher loadings of PbO, i.e., above 4.4% Pb, is likely due to the oxygen-limited reaction conditions resulting from high methane conversion and high CO_x selectivity. This increase in the rate of methane conversion with PbO is indicative of the strong oxidizing nature of PbO and is also reflected in the dramatic increase in the CO_2/CO ratio.

The deactivation behavior of Pb–Mg–O catalysts during methane coupling is different than that reported for other catalytic systems. Whereas catalysts like Sb_2O_4 show an increase in C_2 selectivity with time (*2*), the Pb–Mg–O catalysts showed a decrease in C_2 selectivity accompanied by only slight deactivation. Chemical analyses of the catalysts before and after reaction revealed that, in general, both the surface and the bulk were depleted of the Pb species as a result of the reaction. However, the relative amounts of lead on the surface and on the bulk remained relatively constant suggesting a high mobility of lead species in the catalysts. It is probably because of the rapid replenishment of the surface Pb species, from the bulk of the catalyst, that the catalyst did not show severe deactivation.

The decrease in C_2 selectivity is probably due to the loss of the active Pb species from the catalyst as shown by bulk analysis of the catalysts before and after reaction. It can be speculated that the C_2 selectivity would eventually be comparable with that achieved over bare MgO as lead is lost from the catalyst. In the reducing atmosphere which is employed in methane oxidation, it is not unlikely for an active lead species, such as PbO, to be converted to metallic lead which can be easily lost because of its high vapor pressure.

One question of great importance in oxidative coupling reactions is the chemical nature of the active species. XPS analysis revealed the surface lead to be predominantly in the form of $PbCO_3$. However, since the catalysts were not treated at high temperatures prior to XPS analyses, it is believed that the presence of $PbCO_3$ on the catalyst surface is due to the adsorption of CO_2 from air by PbO. Since $PbCO_3$ decomposes at 315°C, the lead is most likely to exist in the oxide form at reaction temperatures (*26*). It is also possible that during reaction, the CO_2 generated may readsorb on the surface and perhaps form a partial carbonate. However, the exact nature of the lead species, to which we will refer as PbO for convenience, is not critical to the conclusions reached in this work.

Catalysts with low loadings of Pb did not show evidence of any Pb-related X-ray signal in powder diffraction and only a small Pb signal in microscopy analysis. However, XPS measurements of the catalysts did show the presence of Pb on the surface. Thus it can be argued that at low levels of lead, PbO is more-or-less uniformly dispersed on the catalyst surface. Also, XPS analyses indicated an increase in Pb concentration on the catalyst surface with an increase in the bulk Pb content. These findings are corroborated by the STEM results which failed to show the existence of any lead agglomerates at low loadings, thereby suggesting that PbO does in fact exist as a dispersed phase. However, at higher loadings of lead, PbO may exist in two forms: dispersed phase and aggregates.

An increase in the lead content of the cat-

alysts did not lead to an obvious change in the bulk crystal structure of the magnesia, as evidenced by XRD, and no bulk lead–magnesium compounds were formed in detectable amounts even at the highest lead content. Additionally, XPS did not show any measurable change in the phases present on the surface of the catalysts with increasing lead content. Thus, it appears that at low levels, the lead simply disperses over the MgO but remains as PbO or $PbCO_3$. The increase in methane conversion with increasing lead content and the volcano type C_2 selectivity pattern observed as lead is added cannot be ascribed simply to the formation of new phases or to changes in the crystal structure of the Pb–Mg–O catalysts and must be explained by the dispersion of the highly oxidizing PbO over the MgO support.

The effect of PbO on the selectivity to coupled products is interesting. Despite the increased oxidizing ability with increasing PbO, C_2 selectivity actually increased notably for catalysts with low levels of PbO. This type of volcano plot is not unusual in catalytic reactions and can be intuitively interpreted by postulating an "isolated-site" mechanism. When lead is added in small amounts, it disperses over a relatively inert MgO surface resulting in the formation of a number of isolated strong oxidizing sites which can readily abstract a hydrogen from CH_4 and generate methyl radicals with high efficiency. Thus, when methane impinges on these sites the rate of $CH_3\cdot$ radical generation is high and total methane conversion is also high. Moreover, at low PbO content these sites are isolated and the methyl radical has little likelihood of being further oxidized by a neighboring strong oxidizing site and can desorb into the gas phase where it can couple to form ethane. This is reflected in an increase in C_2 selectivity with Pb content, as well as an increase in the methane conversion rate. Further addition of PbO eventually leads to an agglomeration of these strong oxidizing active sites close to each other. This continues to increase the methane conversion rate but now allows for the newly formed $CH_3\cdot$ radical to further oxidize to total oxidation products, thereby decreasing the selectivity for partial oxidation.

Recent studies on the lanthanide oxides have shown that oxides exhibiting multiple oxidation states are ineffective in generating gas-phase $CH_3\cdot$ radicals because of the fast reaction of the $CH_3\cdot$ radicals with the oxide, forming CO_x (*27*). Thus, although PbO has been reported to be less active than MgO for the generation of gas-phase $CH_3\cdot$ radicals from CH_4, it is likely that this is related to the very high activity of PbO which results in the further combustion of $CH_3\cdot$ radicals on the catalyst surface before they can be desorbed into the gas phase (*28*).

Thus, it appears that one requirement for a highly selective coupling catalyst is the presence of strong oxidizing sites but highly diluted within an inert matrix. Such a combination would allow maximum methyl radical generation while controlling the total oxidation due to readsorption and further oxidation of the radicals. The above hypothesis is valid provided the addition of the active oxide does not result in the formation of new phases which might otherwise alter the activity and selectivity behavior.

The idea of isolating the active sites has been proposed to explain the behavior of other partial oxidation processes (*29, 30*). For example, Callahan and Grasselli concluded that for selective oxidation of hydrocarbons the oxygen atoms must be distributed on the catalyst surface in an arrangement which provides for limitation of the number of active oxygen atoms in various isolated groups (*29*). Further support for this hypothesis has been provided by the results of a simple kinetic model which has been developed based on the idea of isolated sites. The model predicts an optimum in C_2 selectivity as a function of Pb content and will be presented as Part II of this work (*31*).

It can perhaps be argued that the specific surface areas of the Pb–Mg–O catalysts

also play an important role in affecting activity and selectivity in methane oxidation. Earlier reports have noted the importance of the specific area of a catalyst during oxidative coupling of methane, indicating that low surface area was conducive to high C_2 yields (*32, 33*). Aika and co-workers concluded that for a given catalyst system an optimum surface area is required to achieve maximum C_2 selectivity (*32*). This is because higher surface area increases the rate of methyl radical formation, but also the rate of radical reaction with the surface resulting in the formation of CO_x. This explanation is somewhat consistent with our results, except that it assumes a constant areal reaction rate which is not the case in the Pb–Mg–O system. While the surface area of the Pb–Mg–O catalysts continuously decreased with increasing Pb content, the areal reaction rate increased and the C_2 selectivity showed a volcano-type relationship. Thus, although an optimum catalyst surface area may indeed be required to achieve the maximum C_2 selectivity, it cannot be explained simply by assuming a constant reactive surface as the lead loading is changed.

In conclusion, the addition of small amounts of an active oxide like PbO to MgO can enhance both the activity and C_2 selectivity in methane oxidation. The increase in C_2 selectivity is believed to be due to the formation of "isolated" sites which reduce the subsequent oxidation of $CH_3\cdot$ radicals on the catalyst. Work is in progress to study the oxidative coupling of methane using other active oxides dispersed on MgO and other supports.

ACKNOWLEDGMENTS

The financial support of the Gas Research Institute is gratefully acknowledged. The authors would also like to acknowledge Dr. J. R. Blachere for his help with the electron microscopy work.

REFERENCES

1. Keller, G. E., and Bhasin, M. M., *J. Catal.* **73,** 9 (1982).
2. Lo, M.-Y., Agarwal, S. K., and Marcelin, G., *J. Catal.* **111,** 168 (1988).
3. Iwamatsu, E., Moriyama, T., Takasaki, N., and Aika, K., *J. Catal.* **113,** 25 (1988).
4. Otsuka, K., Jinno, K., and Morikawa, A., *J. Catal.* **100,** 353 (1986).
5. Emesh, I. T., and Amenomiya, Y., *J. Phys. Chem.* **90,** 4785 (1986).
6. Kimble, J. B., and Kolts, J. H., *Energy Prog.* **6,** 226 (1986).
7. Sofranko, J. A., Leonard, J. J., and Jones, C. A., *J. Catal.* **103,** 302 (1987).
8. Lin, C.-H., Ito, T., Wang, J.-X., and Lunsford, J. H., *J. Amer. Chem. Soc.* **109,** 4808 (1987).
9. Ito, T., Wang, J.-X., Lin, C.-H., and Lunsford, J. H., *J. Amer. Chem. Soc.* **107,** 5062 (1985).
10. Asami, K., Hashimoto, S., Shikada, T., Fujimoto, K., and Tominaga, H., *Chem. Lett.,* 1233 (1986).
11. Hinsen, W., Bytyn, W., and Baerns, M., *Chem. Ztg.* **107,** 223 (1983).
12. Asami, K., Hashimoto, S., Shikada, T., Fujimoto, K., and Tominaga, H., *Ind. Eng. Chem. Res.* **26,** 1485 (1987).
13. Wagner, C. D., Riggs, W. M., Davis, L. E., Moulder, J. F., and Muilemberger, G. E., "Handbook of X-ray Photoelectron Spectroscopy." Perkin-Elmer Corp., Phys. Elect. Div., Eden Praire, 1979.
14. Kim, K. S., O'Leary, T. J., and Winograd, N., *Anal. Chem.* **45,** 2214 (1973).
15. Jorgensen, C. K., *Theor. Chim. Acta* **24,** 241 (1972).
16. Thomas, J. M., and Tricker, M. J., *J. Chem. Soc. Faraday Trans. 2* **71,** 329 (1975).
17. Inoue, Y., and Yasumori, I., *Bull. Chem. Soc. Japan* **54,** 1505 (1981).
18. Yates, D. J. C., and Zlotin, N. E., *J. Catal.* **111,** 317 (1988).
19. Lane, G. S., and Wolf, E. E., *J. Catal.* **113,** 144 (1988).
20. Hutchins, G. J., Scurrel, M. S., and Woodhouse, J. R., *J. Chem. Soc. Chem. Commun.,* 253 (1988).
21. Martin, G. A., Bates, A., Ducarme, V., and Mirodatos, C., *Appl. Catal.* **47,** 287 (1989).
22. Onsager, O. T., Lodeng, R., and Soraker, P., *Catal. Today* **4,** 355 (1989).
23. Roos, J. A., Bakker, A. G., Bosch, H., van Ommen, J. G., and Ross, J. R. H., *Catal. Today* **1,** 133 (1987).
24. Bartek, J. P., Hupp, J. M., Brazdil, J. F., and Grasselli, R. K., *Catal. Today* **3,** 117 (1988).
25. Aika, K.-I. and Nishiyama, T., *J. Chem. Soc. Chem. Commun.,* 70 (1988).
26. "Handbook of Chemistry and Physics," 64th ed. Chemical Rubber Co., Cleveland, Ohio (1983).
27. Tong, Y., and Lunsford, J. H., presented at 11th North American Meeting of the Catalysis Society, Dearborn, MI, 1989.
28. Driscoll, D. J., and Lunsford, J. H., *J. Phys. Chem.* **89,** 4415 (1985).
29. Callahan, J. L., and Grasselli, R. K., *AIChE J.* **9,** 755 (1963).

30. Golodets, G. I., "Heterogeneous Catalytic Reactions involving Molecular Oxygen." Elsevier, NY, 1983.
31. Agarwal, S.K., Migone, R. A., and Marcelin, G., to be published.
32. Iwamatsu, E., Moriyama, T., Takasaki, N., and Aika, K., *J. Chem. Soc. Chem. Commun.,* 19 (1987).
33. Agarwal, S. K., Migone, R. A., and Marcelin, G., *Appl. Catal.* **53,** 71 (1989).